UC Santa Barbara

UC Santa Barbara Previously Published Works

Title

Mechanism for food texture preference based on grittiness

Permalink

https://escholarship.org/uc/item/20m1b7cz

Journal

Current Biology, 31(9)

ISSN

0960-9822

Authors

Li, Qiaoran

Montell, Craig

Publication Date

2021-05-01

DOI

10.1016/j.cub.2021.02.007

Copyright Information

This work is made available under the terms of a Creative Commons Attribution License, availalbe at https://creativecommons.org/licenses/by/4.0/

Peer reviewed

eScholarship.org Powered by the California Digital Library
University of California

Author Manuscript

Author Manuscript

Author Manuscript

Author Manuscript

HHS Public Access

Author manuscript

Curr Biol. Author manuscript; available in PMC 2022 May 10.

Published in final edited form as:

Curr Biol. 2021 May 10; 31(9): 1850–1861.e6. doi:10.1016/j.cub.2021.02.007.

Mechanism for food texture preference based on grittiness

Qiaoran Li[3], **Craig Montell**[3,*]

[3]Department of Molecular, Cellular, and Developmental Biology and the Neuroscience Research Institute, University of California, Santa Barbara, California 93106, USA

Summary

An animal's decision to accept or reject a prospective food is based only in part on its chemical composition. Palatability is also greatly influenced by textural features including smoothness versus grittiness, which is influenced by particle sizes. Here, we demonstrate that *Drosophila melanogaster* is endowed with the ability to discriminate particle sizes in food and uses this information to decide whether a food is appealing. The decision depends on a mechanically-activated channel, OSCA/TMEM63, which is conserved from plants to humans. We found that *tmem63* is expressed in a multidendritic neuron (md-L) in the fly tongue. Loss of *tmem63* impairs the activation of md-L by mechanical stimuli and the ability to choose food based on particle size. These findings reveal the first role for this evolutionarily conserved, mechanically-activated TMEM63 channel in an animal and provide an explanation as to how flies can sense and behaviorally respond to the texture of food provided by particles.

Graphical Abstract

[*]Lead author and lead contact. Correspondence should be addressed to: C.M. (cmontell@ucsb.edu), twitter handle: @CraigMontell1.

Author Contributions

This study was designed by Q.L. and C.M., and directed and coordinated by C.M. All experiments were performed by Q.L. Q.L. and C.M. wrote the initial manuscript draft, and reviewed and edited the manuscript.

Publisher's Disclaimer: This is a PDF file of an unedited manuscript that has been accepted for publication. As a service to our customers we are providing this early version of the manuscript. The manuscript will undergo copyediting, typesetting, and review of the resulting proof before it is published in its final form. Please note that during the production process errors may be discovered which could affect the content, and all legal disclaimers that apply to the journal pertain.

Declaration of Interests

The authors declare no competing interests.

Author Manuscript
Author Manuscript
Author Manuscript
Author Manuscript

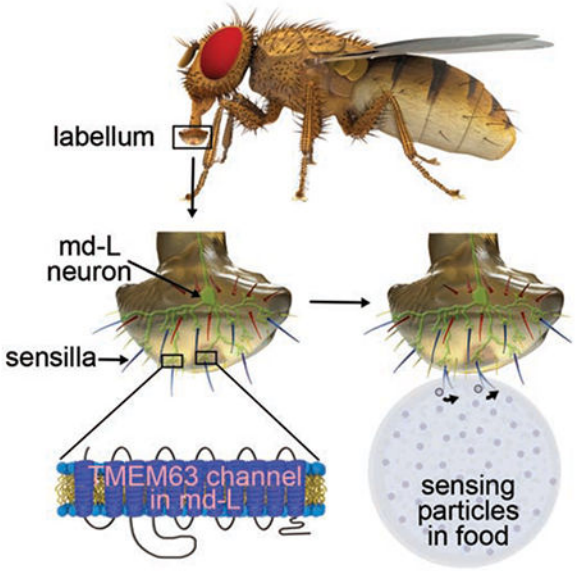

eTOC blurb

In humans the size of particles in food influences palatability. Li and Montell establish that flies also evaluate the size of particles in food and use this information to assess its appeal. Flies discriminate particle sizes in food through mechanical activation of the TMEM63 channel in a multidendritic neuron (md-L) in their tongue.

Keywords

Food texture; gritty; smooth; OSCA; TMEM63; channel; somatosensation; mechanical activation; taste; gustation; particle size; *Drosophila melanogaster*

Introduction

Food selection is among the most critical and ancient behaviors exhibited by animals. Multiple classes of chemosensory receptors have been defined in flies, mice and other animals that contribute to the discrimination of nutritious from noxious foods.[1–3] In humans and other mammals, the textural features of food also have a major impact on food appeal.[4] The texture of food is influenced by its hardness and viscosity, as well as the size of food particles. These features comprise the mouthfeel of food and illustrate the importance of somatosensation for assessing palatability. Nevertheless, the receptors that detect food texture are unknown in mammals. Recently, our group and others have begun to exploit the fruit fly, *Drosophila melanogaster*, to unravel the receptors and neurons that allow animals to evaluate palatability based on physical features of food including hardness,[5–7], viscosity[7] and temperature.[8]

For humans, one of the key physical features of food that impacts food appeal is particle size. For example, ice crystals of 10 to 20 μm cause ice cream to be perceived as very smooth while larger crystals of 50 μm confer a perception of grittiness.[9] Particle sizes in

Author Manuscript Author Manuscript Author Manuscript Author Manuscript

chocolate also influence the evaluation of desirability.[10] In experiments with human volunteers, the addition of garnet, polyethylene or mica particles of different sizes to flavored syrups impacts food appeal.[11]

The influence of particle size on food appeal might be conserved throughout the animal kingdom. *Drosophila* feed on many types of fruit and are especially attracted to ripened and decaying fruit.[12,13] The size of starch granules in mango and kiwifruit range from ~10—15 μm.[14,15] In addition, decaying fruit is laden with yeast, which is also a food source for flies. The size of budding yeast is ~8—10 μm.[16] Thus, flies might prefer foods with particle sizes that are typically found in fruits and budding yeast. However, the underlying molecular and cellular basis through which the size of particles in food alters acceptance or rejection remains unexplored.

Here, we establish *Drosophila* as an animal model for revealing the mechanism through which particle size influences food attraction. We found that flies prefer sucrose-containing food with particles of a particular size. This ability to discriminate between foods based on particle size depends on TMEM63, a member of a recently-discovered family of mechanically-activated channels that are conserved from plants (OSCA) to animals including humans (TMEM63).[17–20] OSCA/TMEM63 represents the only protein family shown to be mechanically-gated ion channels in both plants and animals.[20] However, their roles in animals are unknown. We found that the role of TMEM63 in sensing particles in food is dependent on its expression in a pair of mechanically-activated multidendritic neurons (md-L) in the labellum, which is the fly's major taste organ. While TMEM63 is required for sensing small particles in food, which exert subtle mechanical forces, it is dispensable for detecting other textural features of food such as hardness and viscosity, which cause stronger mechanical interactions with the labellum. Another mechanosensitive channel, TMC, is also expressed in md-L neurons.[7] However, in contrast to TMEM63, the TMC protein functions in detecting the hardness and viscosity of food[7] but is dispensable for particle sensation. Our results reveal the first molecular and cellular underpinning for sensing particle sizes in food, and a requirement for a TMEM63 channel in an animal.

Results

Particle size influences food appeal in flies

To monitor a fly's motivation to feed, we used the proboscis extension response (PER).[8,21] If the labellum is touched with an appealing food at the end of a probe, the animal will extend its proboscis in an attempt to feed. The interest in feeding increases with the starvation time. A PER is scored as 1.0 if the fly extends its proboscis for ≥1 second, while the PER is 0.5 if the animal extends its proboscis <1 second. If there is no PER, then the score is 0. To obtain a modest PER, we briefly starved the flies (2 hours) and then offered them a relatively low level of sugar (50 mM sucrose). Consequently, the flies exhibited a PER score of only 0.35 ±0.04. Because the size of food particles imparts textural features such as smoothness and grittiness and affects palatability in humans, we wondered whether the addition of particles of different sizes to sucrose would also impact food appeal to flies. To address this question, we used particles of defined size and that would affect only the texture and not the chemical composition of the food. Therefore, we added different sizes of silica microspheres to 50

Author Manuscript Author Manuscript Author Manuscript Author Manuscript

mM sucrose while maintaining a constant 10% weight/volume. We used particles in the 1—30 μm range since many of the granules in foods consumed by flies are in the 5—15 μm range.[14–16]

We found that adding particles to sucrose had a major effect on its appeal. Introduction of the smallest particles tested (1 μm) significantly increased the PER, and inclusion of 9.2 μm particles resulted in a profoundly higher PER score (0.77 ±0.05; Figures 1A—1D). 20 μm particles had a smaller positive influence, which was similar to the effect of 1 μm particles (Figure 1D). The benefit of particles on food attraction was erased by 30 μm microspheres since this elicited PERs similar to sucrose alone (Figure 1D). Thus, 9.2 μm particles enhance food attraction to the greatest extent. When we adjusted the percent of 9.2 μm particles in the sucrose, the PER reached a peak at 10% (Figure 1E). While 10% 9.2 μm particles increased the likelihood of exhibiting a PER, it did not increase the average ingestion time per PER relative to sucrose alone (Figure 1F).

To test whether this added attraction was due to the particles and not a chemical released from the particles we incubated 10% 9.2 μm particles in 50 mM sucrose for 30 minutes, removed the particles by centrifugation and performed PER assays. The PERs were indistinguishable from the responses using 50 mM sucrose that was not pre-exposed to the particles indicating that a released chemical was not the basis for the increased PER resulting from addition of the 10% 9.2 μm particles (Figure 1E). Therefore, we focused on 10% 9.2 μm particles for our subsequent experiments.

To determine the interplay between sucrose concentration and the texture created by particles, we varied the levels of sucrose. In the absence of sucrose (0 mM), there was virtually no PER, even in the presence of 9.2 μm particles (Figure 1G). Thus, particles without nutrient content is not sufficient to trigger feeding behavior. Similarly, the minimal PER produced by 10 mM sucrose was not significantly increased by the addition of particles. In striking contrast, when we offered flies either 50 mM or 100 mM sucrose, the particles greatly increased the PERs (Figure 1G). The impact of particles on the appeal of 50 mM sucrose was so profound that it caused it to be as attractive as 200 mM sucrose alone (Figure 1G). Particles had less of an effect when presented with 200 mM or 500 mM sucrose, since the sucrose-only PER was already high at these concentrations (0.84 ±0.02 and 0.98 ±0.01, respectively; Figure 1G). When we starved flies for 16 hours, thereby increasing their PER to 10 mM sucrose, the particles enhanced the appeal of this low level of sugar (Figure 1H). Thus, the impact of particle texture on feeding was not strictly due to the concentration of sucrose. Rather, it occurred when there was an intermediate level of sucrose attraction, which could be also achieved at a low sucrose concentration (10 mM) if the starvation time is increased. The effect of 10% 9.2 μm particles on feeding did not appear to be due to changes in viscosity since the presence of particles on the viscosity of 50 mM sucrose was negligible (Figure S1A).

tmem63 required for discriminating particle size in food

To investigate the molecular mechanisms underlying the sensation of particle size in food, we tested the effects of mutations disrupting several known mechanosensitive channels including PIEZO,[22], TMC,[7] NOMPC[23], Iav,[24] and Nan.[25] These mutants showed increased

Author Manuscript Author Manuscript Author Manuscript Author Manuscript

PERs to food with particles similar to the control (Figure 2A), although one of the two *iav* alleles (*iav*^{3621}) showed a slightly diminished response, which was not exhibited by the other allele *iav*^{1} (Figure S2A) or the trans-heterozygous flies (*iav*$^{1/3621}$; Figure 2A). Therefore, none of these channels are essential for detecting the texture provided by particles.

To identify a channel that might be critical for sensing particles in food we considered the fly homolog of the mechanosensitive OSCA/TMEM63 channel[19,20] (Figures S1B—S1D). To interrogate a requirement for *tmem63*, we generated two mutant alleles. The *tmem63*^{1} mutation removed the first 3 out of 11 transmembrane domains (TMD0-2), while the mutation in *tmem63*^{2} deleted the last two transmembrane domains (TMD9-10). Both *tmem63*^{1} and *tmem63*^{2} were viable. In response to sucrose alone the mutants showed normal PERs (Figure S2B). However, in contrast to control flies, particles did not increase sucrose attraction (Figure 2A). These data indicate that TMEM63 is essential for sensing particles in food. Loss of *tmem63* did not impact the ability to detect the viscosity (modified with HPC) or hardness of a sucrose-containing food (modified by adding agarose; Figure 2B).

The ability of the mutants to detect other tastants tested, including tartaric acid, NaCl and caffeine, was indistinguishable from the controls (Figures S2C—S2E). We found that the moderate declines in sucrose attraction by 1% tartaric acid or 250 mM NaCl were suppressed by the 9.2 μm particles in control flies but not in *tmem63*^{1} (Figures 2C and 2D). In addition, the reduction in PER upon addition of 10 mM caffeine to sucrose was reversed by particles in control flies but not in *tmem63*^{1} (Figure 2E). However, the near complete inhibition of sucrose attraction by 100 mM caffeine was not reduced by particles (Figure S2F). Thus, mild avoidance of a low level of an aversive compound can be reversed by particles, but not the severe avoidance due to high concentrations of the same aversive chemical. These data support the conclusion that 9.2 μm particles elicit attraction and can counter the negative effects of mildly aversive chemicals on sucrose appeal.

Expression of *tmem63* in the labellum

The demonstration that *Drosophila* TMEM63 is a mechanically-activated channel[20] and is required for particle sensation suggests that it might be expressed and function in mechanosensory neurons (MSNs). The main gustatory organ in flies is located at the end of the proboscis and consists of two bilaterally symmetrical labella. Each labellum is comprised of 31 taste sensilla with external hairs and two or four gustatory receptor neurons (GRNs), a pair of short sensilla on the lateral side that appear to be poreless, mechanosensory (PM) sensilla and 30—40 conically shaped hairless sensilla (taste pegs) with one GRN.[26,27] The taste hairs and pegs also contain one associated MSN (hMSN and pMSN, respectively). In addition, each labellum harbors one mechanonsensitive multidendritic neuron (md-L), which extends dendrites to the bases of ~70% of taste hairs.[7]

To examine the expression of *tmem63* in the labellum we used CRISPR/Cas9 to knock in a reporter so that it expressed under the endogenous transcriptional and translational control of *tmem63*. We inserted DNA encoding *P2A::Gal4* in place of the stop codon at the end of the *tmem63* gene. Due to the P2A peptide, the Gal4 protein is released during translation. We found that the *tmem63-PGal4* labeled multiple neurons including one that appeared to be

Author Manuscript Author Manuscript Author Manuscript Author Manuscript

md-L (Figure 3A). We confirmed that the *tmem63-PGal4* stained md-L by performing double labeling with the *tmc-QF* reporter, which defines the md-L neurons[7] (Figure 3A—3C). We performed *in situ* hybridizations and found that the *tmem63* probe labeled md-L from labella dissected from control flies but not from *tmem63*^{1} (Figures S3A—S3F).

In addition to md-L, the *tmem63-PGal4* reporter labeled many other neurons associated with external taste sensilla, taste pegs and the two PM bristles. We performed double-labeling to identify the proportion that are MSNs and other types of neurons. The MSN reporter (*nompC-LexA*) labels 65 ±0.8 neurons (Figure 3E, Table 1: hMSNs, 30.0 ±0.5; pMSNs, 33.3 ±0.3; pmMSNs, 2.0 ±0.0).[5] There was no overlap between the *tmem63-PGal4* and *nompC-LexA* in any of the 31 external taste sensilla (hMSNs; Figures 3D—3F, Figures S3G—S3J, and Table 1). However, both of the PM bristles (pmMSNs; Figures 3D—3F, Figures S3K—S3N) and 6.0 ±0.6 taste pegs were labeled by both reporters (pMSNs; Figures S3O—S3Q and Table 1). To identify the type of GRNs that express *tmem63* we conducted additional double-labeling experiments. S- and L-type sensilla contain four GRNs while I-type sensilla contain two GRNs.[1] Most GRNs respond to multiple stimuli but for simplicity are referred to as: (A) sweet, (B) bitter, (C) water, (D) cation, and (E) low salt.[1] All A—D GRNs appeared to express the *tmem63* reporter (Figures 3G—3R and Table 1). We did not examine overlap with E GRNs, which are specific to L-type sensilla, since the only available reporters are *Gal4* lines. Thus, *tmem63* is also expressed in most GRNs but in very few MSNs in S-, I- or L-type taste sensilla or MSNs in pegs.

tmem63 required in md-L neurons for attraction to particles in food

The observations that *tmem63* is expressed in multiple types of neurons raised the question as to which type functions in detecting particles in food. Therefore, we inactivated synaptic transmission in different classes of neurons by expressing a tetanus toxin transgene (*UAS-TNT-E*) under the control of a variety of *Gal4* drivers. The *UAS-TNT-E* was effective since expression of this transgene in A GRNs using the *Gr64f-Gal4* eliminated PERs to sugar (Figure 4A). However, it is not possible to interrogate a contribution of A GRNs to particle sensation since the *UAS-TNT-E* inhibits the sugar response of these neurons. Inactivating MSNs in taste hairs and pegs (hMSNs and pMSNs) or B, C, D or E GRNs did not blunt the flies' increased attraction to sucrose containing particles (Figures 4A and 4B). Thus, none of these MSNs or GRNs are essential for sensing the texture of particles in food. In contrast, when we expressed *UAS-TNT-E* in md-L neurons under using the *tmc-Gal4*, particles did not increase the appeal of sugar (Figure 4A) indicating that md-L neurons are crucial for this response. In addition, we rescued particle sensation in *tmem63* mutants by expressing *UAS-tmem63* under control of the *tmc-Gal4* (Figure 4C).

We also tested whether we could rescue the *tmem63* mutant phenotype using a *tmem63-Gal4* that expressed *Gal4* under the control of a 3 kb genomic sequence flanking the 5' end of *tmem63*. We used the *tmem63-Gal4* for the rescue experiments since it has a more limited expression pattern than the *tmem63-PGal4*, which we knocked into the 3' end of the *tmem63* coding region. While the *tmem63-Gal4* was expressed in md-L (Figure 4D—4F) similar to the *tmem63-PGal4*, the *tmem63-Gal4* was expressed in less than half as many other neurons (Figure S4A; Table 1, ~53 neurons) in the labellum as the *tmem63-PGal4*

Author Manuscript Author Manuscript Author Manuscript Author Manuscript

(Figures 3D; Table 1, ~134 neurons). Most of the *tmem63-Gal4-positive* neurons are B and D GRNs (Figures S4G—S4I, S4M—S4O and Table 1) and peg GRNs (Figures S4P—S4R and Table 1). As with the *tmc-Gal4*, we rescued the *tmem63* mutant phenotype using the *tmem63-Gal4* to drive expression of *UAS-tmem63* (Figure 4C).

We showed previously that *tmc* is required in md-L neurons for sensing other textual features of food—hardness and viscosity.[7] However, as mentioned above, *tmc* is not required for sensing particles in food (Figure 2A) and *tmem63* is not needed for detecting hardness and viscosity (Figure 2B). Thus, *tmem63* and *tmc* are required in md-L neurons for detecting different textural qualities in food.

tmem63 is critical for sensing moderate deflections of taste sensilla

The sensation of particles in food by md-L neurons might be mediated by deflection of sensilla. Therefore, we added 10% 9.2 μm particles to 50 mM sucrose and monitored the deflection angles after <0.2 seconds of contact with the labellum. We focused on L-type sensilla since the dendrites from the md-L neurons extend into ~70% of the sensilla including most L-type sensilla and only one S-type sensillum (S6). Within the field of view we were able to quantify deflection angles from 4.0 ±0.3 L-type sensilla that were in contact with the liquid (Figures S5A and S5B). In the presence of sucrose only (clear food) the sensilla were deflected 4.5° ±0.7° (Figure 5A). Upon application of food with 1.0 μm and 9.2 μm particles (particle food) there were wider distributions of deflection angles. Some showed small deflections in the range similar to the sucrose alone, while the remaining sensilla exhibited greater deflection angles. 1 μm particles caused an increase to 8.0° ±1.1° and 9.2 μm particles increased the average deflections to 13.8° ±2.0° with a maximum of ~30° (Figures 5A and S5B).

To determine whether *tmem63* is required for md-L neurons to sense deflections of multiple sensilla in a range similar to that caused by particles in sucrose, we devised an approach to deflect multiple bristles. We used a sealed tapered glass pipet to poke the cuticle of the labellum between the bases of the L8 and S6 sensilla (Figure 5B). As we increased the cuticle deformation (10—40 μm; steps I—IV) the number of affected sensilla increased from four to eight (L-type and S6; Figure 5C). We focused on L3 and L4 sensilla and found that the deflection angles produced by deformations of up to 30 μm (steps I—III) were similar to those produced by particles (Figures 5A and 5C). The average deflection angles caused by 1.0 μm particles in food (8.0° ±1.1°) were intermediate between the average bending angles produced by the 10 μm and 20 μm cuticle deformations (steps 1 and 2, respectively; Figures 5A and 5C). The larger deflections caused by the 9.2 μm particles (13.8° ±2.0°; Figure 5A) were slightly larger than the step 2 cuticle deformation (12.5° ±2.0°;5C). The 40 μm deformation (step IV) caused deflections greater than that produced by the particles (Figures 5A and 5C).

To monitor the responses of md-L neurons we used a genetically encoded fluorescent Ca^{2+} sensor (*UAS-GCaMP6f*) expressed under control of the *tmc-Gal4*. We co-expressed *UAS-tdTomato* since tdTomato fluorescence is not impacted by Ca^{2+}. We poked the cuticle to cause deflections of the sensilla as described above (steps I—IV) and monitored the changes in fluorescence ($\Delta F/F_0$). The dtTomato fluorescence in the md-L neurons changed very little

Author Manuscript Author Manuscript Author Manuscript Author Manuscript

during the cuticle deformations indicating that any change in GCaMP6f fluorescence was unlikely to be due to movement artifacts (Figures 5D, 5F—5J). We found that md-L neurons in control animals responded to 10 μm deflections (step I; Figures 5D, 5E and 5G). The responsiveness increased up to 30 μm (steps II and III), and then plateaued (step IV; Figure 5D, 5E and 5G).

We found that the mechanically-induced GCaMP6f responses of md-L neurons in *tmem63* mutants were diminished greatly. The $\Delta F/F_0$ due to the 10 and 20 μm steps were eliminated and the response to the 30 μm step was minimal (Figures 5E, 5F and 5H). However, the *tmem63* mutant md-L neuron responded to the 40 μm step, although it was reduced relative to the control (Figures 5E, 5F and 5H). We rescued the *tmem63* phenotype by expressing *UAS-tmem63* using the *tmc-Gal4* (Figures 5E and 5I). These data further support the conclusion that *tmem63* functions in md-L neurons. The tmc^1 mutant also showed a reduced response to the various steps; however, the deficit was not as great as exhibited by the $tmem63^{1/2}$ mutant (Figures 5E and 5J).

To determine whether *tmem63* is required for mechanically-induced action potentials in md-L neurons we performed single unit recordings by impaling a recording electrode near the cell body of md-L. A 10 μm or 20 μm indentation of the cuticle in control labella induced a transient burst of action potentials that lasted for 202 ±22 and 383 ±41 milliseconds, respectively (Figures 5K—5M). The activity was virtually eliminated in the *tmem63* mutant and was rescued by expression of *UAS-tmem63* under control of the *tmc-Gal4* (Figures 5K—5M). Thus, *tmem63* is required for mechanically-induced action potentials in md-L neurons. Action potentials were still generated although they were significantly reduced in tmc^1 in response to the 10 μm and 20 μm indentations of the cuticle (Figures 5K—5M). However, the 10 μm indentation did not produce a GCaMP6f response (Figure 5E) indicating that the field recordings afforded greater sensitivity.

The cuticle indentation protocol permits us to assess the responses of md-L neurons to deflections of multiple bristles that move within a short time interval. We then monitored the GCaMP6f responses of md-L neurons to deflections of a single sensillum. We focused on the L7 sensillum since it is among the ~70% of the sensilla innervated by md-L dendrites (Figure S5C) and is easily accessible to mechanical manipulation (Figures S5D—S5H). When we deflected the L7 sensillum 5 μm, 20 μm; or 50 μm, the $\Delta F/F_0$ from the control increased with the larger deflections (Figures S5I—S5M). However, when we deflected L7 from $tmeme63^{1/2}$, the responses to the smaller deflections (5 μm and 20 μm) were eliminated (Figures S5I, S5J, S5N and S5O), while there was no significant difference from the control when we bent the L7 sensillum 50 μm (Figure S5K). In contrast to $tmem63^{1/2}$, the smaller movements of L7 (5 μm and 20 μm) from the tmc^1 labellum induced similar GCaMP6f responses as the control (Figures S5I, S5J, S5P and S5Q). However, the tmc^1 response to the 50 μm deflection of L7 was significantly reduced (Figure S5K).

Discussion

Mouthfeel results from the physical features of food including hardness, viscosity, and particle size. The human gustatory experience is influenced by particle size since it impacts

Author Manuscript Author Manuscript Author Manuscript Author Manuscript

on whether a food is smooth or gritty. But the mechanisms are unknown. We established that flies are also able to discriminate between food based on particle size. Their favorite size was 9.2 μm, which falls within the size range of the budding yeast in their diet and the starch granules in many of the fruit that they consume.[14–16] The width of their pharynx is ~15 μm. Thus, there might be a selection for a preference for particles <15 μm. However, the width of the pharynx may not define the upper size limit of particles. While flies do not chew food they can process food extra-orally by expelling enzymes from the proboscis.[28]

The sensation of particle size in food is a type of somatosensation, which we propose depends on the detection of particles physically interacting with gustatory sensilla. Deflection of sensilla then activates a mechanically-activated channel in md-L neurons that is critical for particle sensation. In support of this model, particles in food cause small deflections of gustatory sensilla. When we depressed the cuticle with a probe, thereby resulting in small angle deflections similar to those produced by particles, the md-L neurons displayed increased GCaMP6f responses and action potentials.

We found that the mechanically-activated channel is TMEM63 since loss of this channel impairs food discrimination based on particle size. TMEM63 is expressed in md-L neurons and mutation of *tmem63* disrupts activation of md-L neurons by deflection of taste sensilla. Another mechanically-activated channel, TMC, is also required in md-L neurons but for different aspects of texture sensation: hardness and viscosity.[7] The overall structure and dimeric composition of OSCA/TMEM63 channels is similar to the structure and dimeric architecture of TMCs.[19,29–31] Thus, this common structure may be well suited for sensing small physical differences in food texture.

Despite the structural similarities and co-expression of TMEM63 and TMC in md-L neurons, we suggest that it is unlikely that TMEM63 heterodimerizes with TMC. Expression of *Drosophila* TMEM63 *in vitro* is sufficient to produce a mechanically-activated channel.[20] Moreover, the phenotypes of *tmem63* and *tmc* mutants are distinct. While loss of *tmem63* disrupts particle size sensation, the mutants can still discriminate between sugary foods with differences in hardness and viscosity. Conversely, mutation of *tmc* impairs the ability to detect the hardness and viscosity of sucrose-containing food but does not alter the behavioral preference for sucrose with particles.

The observations that flies can discern different textural feature of food such as hardness from particle size raises questions concerning the coding mechanism. This issue is particularly provocative given that the md-L neuron functions in the detection of these distinct textural features. We suggest that one potential explanation is that md-L as well as the MSNs that are associated with each taste hair are all required for the detection of food hardness and viscosity, while only the md-L neuron functions in particle size discrimination. Indeed, hMSNs also contribute to food hardness detection.[5,6]

Alternatively, but not mutually exclusive is that TMEM63 and TMC function in sensing different levels of deflection of gustatory hairs. The responses of md-L neurons to smaller deflections of a single sensillum are eliminated by the *tmem63* mutation but not impacted by the *tmc* mutation. Conversely, the responses to larger deflections are impaired by the *tmc*

Author Manuscript Author Manuscript Author Manuscript Author Manuscript

mutation but not the *tmem63* mutation. This suggests that TMC is required for larger mechanical stimulation caused by hard and viscous food, while TMEM63 is critical for more subtle mechanical stimulation that mimics the effects of particles in food. Indeed, TMEM63 could even provide md-L neurons with sensitivity to the smallest particles tested (1 μm), since 1 μm particles in food elicit small deflections of sensilla that are intermediate between those produced by the steps 1 and 2 cuticle depressions that induce action potentials in control but not *tmem63* mutants.

It is also plausible that there are differences in the spatial and temporal deflections due to hardness/viscosity versus particles. Particles would cause only some adjacent sensilla in any group to be transiently deflected at any given time as they are contacted by the particles. In contrast, hardness/viscosity would result in neighboring sensilla (e.g. L-type) to be simultaneously deflected. In addition, TMEM63 may be more rapidly inactivated than TMC, enabling TMEM63 to be better suited to sense transient deflections from particles. However, a direct comparison between TMEM63 and TMC is not possible since most TMCs including fly TMC has been refractory to biophysical analyses *in vitro*.

The finding that *tmem63* is expressed in many GRNs raises future questions as to the roles of TMEM63 in GRNs. We found that the GRNs do not function in particle sensation and mutation of *tmem63* does not cause defects in sensation of sucrose, caffeine, a carboxylic acid or NaCl. Finally, this and our previous study on TMC[7] raises questions as to whether TMEM63 and TMC function in food texture sensation in mammals.

STAR Methods

RESOURCE AVAILABILITY

Lead Contact—The lead contact is Craig Montell (cmontell@ucsb.edu).

Materials Availability—All unique/stable reagents generated in this study are available from the Lead Contact without restriction. The fly stocks generated in this study will be deposited with the Bloomington Stock Center for public distribution (http://flystocks.bio.indiana.edu/). Further information and requests for resources and reagents should be directed to and will be fulfilled by the Lead Contact.

Data and Code Availability—This study did not generate any unique datasets or code.

EXPERIMENTAL MODEL AND SUBJECT DETAILS

Fly stocks and husbandry—All experiments were performed with the indicated strains of adult male and female *Drosophila melanogaster*. Flies were reared at 25°C on normal cornmeal/molasses food under 12 hr light/12 hr dark cycles. Unless indicated otherwise, all the flies were 3—5 days old and were transferred to fresh vials at a density of 30—50 flies per vial after eclosion. The control flies were w^{1118}. All the mutants were backcrossed into the w^{1118} background for five generations.

The sources of the following flies were: *Gr66a-Gal4* (chromosome 2 insertion, from H. Amrein), *Gr66a-Gal4* (chromosome 3 insertion) (Bloomington Stock 57670), *Gr64f-Gal4*

Author Manuscript Author Manuscript Author Manuscript Author Manuscript

(Bloomington Stock 57669), *ppk28-Gal4*,[33] *ppk23-Gal4*,[34] *Ir94e-Gal4* (Bloomington Stock 81246), *TMC-Gal4*,[7] *TMC-QF*,[7] *QUAS-Gal4* (on III chromosome, isolated from Bloomington Stock 83132), *UAS-TNT-E*,[35] *QUAS-mtdTomato* (Bloomington Stock 30004), *UAS-tdTomato* (Bloomington Stock 36327), *UAS-GCaMP6f* (Bloomington Stock 42747), *nompC-lexA* (Bloomington Stock 52241), *LexAop-rCD2::RFP* (Bloomington Stock 67093), *LexAop-TNT* (a gift from Chi-Hon Lee), *UAS-GFP* (Bloomington Stock 52261), $nompC^{3}$,[23] $nompC^{4}$,[23] $nompC^{f00642}$ (Bloomington Stock 85609), $piezo^{KO}$ (Bloomington Stock 58770), iav^{3621},[24] iav^{1} (Kyoto Stock Center 101174), nan^{36a},[25] *Gr64f-LexA*,[36] *ppk23-LexA* (a gift from Dr. Barry Dickson), *ppk28-LexA*,[37] and *Gr66a-I-GFP*,[38] *Ir76b-QF*.[7]

METHOD DETAILS

Proboscis extension response (PER) assays—We prepared flies for the PER assays as described.[8] Briefly, we starved males for 2 hrs for the assays, unless indicated otherwise, and trapped the animals in a cutoff pipet tip (Olympus 200 μL Reach Tip, 24-150RL) with only the labellum exposed. We water saturated the flies before stimulating them with the food (0.5 μL in volume) for ~0.2—0.6 sec on the labellum. We scored the responses as follows: 1—fly fully extended its proboscis and consumed food ≥1 sec, 0.5—fly extended its proboscis and consumed food <1 s, and 0—fly failed to extend its proboscis. Each trial (n=1) included ≥ 12 flies. The PER index per trial was calculated as: (sum of the score)/(number of flies tested) x 100%. The particles (monodisperse silica microspheres; Cospheric, Co.) were added to the liquid food and mixed thoroughly by pipetting immediately before offering the food to flies.

Generating *tmem63* mutant lines—To generate the null $tmem63^{1}$ mutant, we used ends-out homologous recombination[39] to replace the first three transmembrane segments (sequences 16—1026) with an insertion consisting of *mini white* and an out of frame *Gal4*. To generate the construct for the knockout, we prepared genomic DNA from w^{1118} and PCR amplified a 2890 and a 2983 base pair DNAs arm flanking the 5' and 3' ends of the deleted region using the following primers:

forward primer for 5' arm: CAGGAGCAGGTCGTTCACAACATTC, reverse primer for 5' arm: TTCCGACATGACCATGAATTTCACTA; forward primer for 3' arm: AGAACGCCTACGAATATTATCAGCG, reverse primer for 3' arm: TATGCTGCGTGCTCAATTCGATGCGG.

Each arm was then inserted into the pw35 *Gal4* vector.[40] The donor flies were obtained by germ line transformation of w^{1118} flies (Bestgene, Inc., Chino Hills, CA, USA). We picked donor flies with an insertion on the 3rd chromosome and crossed them to *70FLP,70I-SceI/* TM3,*hs-hid* line (Bloomington Stock 25679) to excise the targeting construct from the genome. F1 progeny with mosaic-eyes were crossed to w^{1118} to obtain red-eyed F2 progeny. We selected F2 progeny with the transgenic components on the 2nd chromosome (~1 %) and confirmed the genotype by PCR. The *Gal4* was not expressed in this line because it was inserted out of frame 23 base pairs after the *tmem63* start codon.

To generate the $tmem63^{2}$ mutant, we used CRISPR/Cas9 to replace the region encoding the 10th and 11th transmembrane domains (1965—2285) with the *LexA* and *mini white* (w^{+})

Author Manuscript Author Manuscript Author Manuscript Author Manuscript

genes. The donor plasmid was pBPLexA::p65Uw. The two homology arms were amplified from genomic DNA prepared from w^{1118} flies using the following primers:

forward primer for 5' arm: CATGGTCATGTCGGAAAACAGCAAC, reverse primer for 5' arm: GGTGCCGCAGAACCGTAAACAA; forward primer for 3' arm: AGAACGCCTACGAATATTATCAGCG, reverse primer for 3' arm: TGCGTGATATCATGTTTGACGGACCG.

The 5' arm was inserted between the AatII and Acc65I sites, and the 3' arm was inserted into the NdeI site. The two guide-RNA targeting site sequences were GTCAAACATGATATCACGCA and GTCGTACTCGGACACGCTGT.

Generating *tmem63* reporters—We used CRISPR/Cas9 to generate the *tmem63-PGal4* reporter line, which consisted of the sequences encoding P2A::Gal4, which were inserted in frame in place of the TAA stop codon. The construct also included an insertion of the *mini-white* (w^+) gene. The donor plasmid (provided by Junjie Liu) was pw35*Gal4* that was modified by fusing the *P2A* self-cleavage sequence (GCCACCAACTTCAGCCTGCTGAAGCAGGCCGGCGATGTGGAGGAGAACCCCGG GCCC) 5' to the *Gal4* start site. The two homology arm was amplified from w^{1118} genomic DNA using following primers:

forward primer for 5' arm: CACCTGATGGCTGTAATGGCATTG, reverse primer for 5' arm: CGCCTCAACACTGTTGACGCTGTA; forward primer for 3' arm: CTGCACGCGAAAGCGATAGCAAT, reverse primer for 3' arm: GATTACTTGTGGGCAAATCGGCATC.

The two guide-RNA targeting site sequences were GGCGTAAATGGTATTATTG and GCTATCGCTTTCGCGTGCAG.

The *tmem63-Gal4* transgene was inserted on the 3rd chromosome and was composed of *Gal4* expressed under control of a 2.89 kb *tmem63* promotor (nucleotides −2875 to +15; +1 is the predicted start site of transcription). *UAS-tmem63* is a 3rd chromosome insertion, which was constructed by subcloning the entire *tmem63* coding region from the *CG11210* cDNA (nucleotides +1 to +2283; +1 is the starts site of translation) into the pUAST plasmid. The primers for cloning the cDNA were:

forward primer: ATGGTCATGTCGGAAAACAGCAACA

reverse primer: TTACGCCTCAACACTGTTGACGCT.

Immunostaining—All immunostaining was performed using whole mount preparations of labella, and the images were acquired using a Zeiss LSM 700 confocal microscope. Briefly, labella were removed with fine scissors (Vannas Spring Scissors, 15001-08) and fixed in 4% paraformaldehyde (Electron Microscopy Sciences) and 0.2% Triton X-100 in 1x PBS for 0.5 hr. The samples were washed 3 times in washing buffer (0.2% Triton X-100 in 1x PBS) and blocked for 1 hr in washing buffer containing 5% normal goat serum. The samples were then incubated with primary antibodies for 1 day at 4°C in 0.2% Triton X-100 and 5% normal

Author Manuscript Author Manuscript Author Manuscript Author Manuscript

goat serum in 1x PBS. After washing 3 times for 1 hr each, the tissues were incubated for 2 hrs at room temperature with secondary antibodies diluted in 0.2% Triton X-100 and 5% normal goat serum in 1x PBS. After 4 washes (0.5 hr each), the labella were mounted on glass slides with VECTASHIELD anti-fade mounting media (Vector Labs, catalog. H-1200). Primary antibodies: anti-GFP (mouse, 1:200, Invitrogen, A-11120), and anti-DsRed (rabbit,1:200, Takara Bio #632496). Secondary antibodies: Alexa Fluor 488 conjugated goat anti-mouse (1:200, Thermo Fisher Scientific, A-11001), and Alexa Fluor 568 conjugated goat anti-rabbit (1:200, Thermo Fisher Scientific, A-11036).

mRNA *in situ* hybridizations—*In situ* hybridizations were performed as previously described[41] with minor modifications. Briefly, to create the template used to generate the digoxigenin-labeled RNA probe, we subcloned the 2,283 nucleotide cDNA encoding the full *tmem63* coding region between the XbaI and BamHI sites of pCS2P+ (Addgene, #17095). We then linearizing the pCS2P-c*tmem63* plasmid with BamHI and prepared the RNA probe by transcription with T7 transcriptase (DIG RNA Labeling Kit, Roche, # 11175025910). We dissected the labellum and introduced an ~50-100 μm opening for the reagents to penetrate. We fixed the samples in 0.2% Triton X-100 in 1x PBS (PBST) for 0.5 hr, washed in PBST 5 times for 10 min each, and incubated in Hybridization solution (HYB) overnight at 60°C. The HYB consisted of 50% v/v formamide (Sigma, #F9037), 5xSSC (Thermo Fisher, #AM9770), 50 μg/mL heparin (Sigma, #H3393-10KU), 0.1% Tween 20 (Sigma, #P9416), 100 μg/mL tRNA (Thermo Fisher, #15401029) and 100 μg/mL sheared, boiled salmon sperm DNA (Sigma, #D1626) in DEPC treated water (Thermo Fisher, #AM9920). We then incubated the samples with the RNA probe (final concentration: ~1 ng/μL) at 56°C overnight, washed in HYB for 20 min at 56°C, washed in 50% HYB, 50% PBST for 20 min at 56°C, washed in PBST 5 times for 10 min each, blocked in blocking buffer for 1 h at room temperature, incubated in biotin-conjugated digoxigenin primary antibody (1:100, Jackson ImmunoResearch Laboratories, #200-062-156) at 4°C overnight, and washed in PBST 5 times for 10 min each. The signal was detected using the Tyramide Signaling Amplification method by following the protocol in the kit (Thermo Fisher, #40932), using a 10 min reaction time. The md-L neuron was distinguished from other neurons on the basis of the large nucleus.

GCaMP6f imaging—To visualize intracellular Ca^{2+} dynamics in live animals, we expressed *UAS-GCaMP6f* in md-L neurons under control of the *tmc-Gal4*.[7] As a control to normalize the data, we also expressed *UAS-tdTomato* in the same neurons. To perform the analyses, we prepared samples as described previously.[8] Briefly, fly heads were cut with fine scissors in 1xPBS. After allowing the samples to recover for 2—5 minutes (until the proboscis was extended and the two labia were in a closed state), we sealed the cut area on the neck with silicone lubricant (Dow Corning, DC 976 High Vacuum Grease). The extended labellum was immobilized on a drop of silicone lubricant and covered with 1xPBS.

To stimulate the samples, we applied different levels of force to the labellum using a pulled glass pipet (World Precision Instruments, 1B150F-3) and fire sealed the end (1-3 μm diameter). The glass pipet was mounted on a shaft held by a motorized micromanipulator (Scientifica PatchStar), which we controlled using Linlab 2 software (Scientifica PatchStar).

Author Manuscript Author Manuscript Author Manuscript Author Manuscript

The md-L neurons dendrites extend into the S6 sensilla and all L-type sensilla. To indent the cuticle, we positioned the pipet to push in between the base of L8 and S6 (Figure 5B) for various distances (~10, 20, 30 and 40 μm). The labella used for these experiments were responsive to the stimuli for ≥30 min.

To deflect a single sensillum (L7), we used a blunt glass probe with a ~40 μm opening, and positioned it at the distal end of the L7 hair. We then deflected the single L7 hair by moving the probe with a motorized micromanipulator (Scientifica PatchStar) and measured the deflection distance using Zeiss confocal software. A typical L7 is marked in the z stacked image of labellum (Figure S5C).

We performed the imaging using a Zeiss LSM 700 confocal microscope under a 20x water immersion objective. GCaMP6f fluorescence signals were normalized to the tdTomato. The traces showing the Ca^{2+} kinetics or the tdTomato control are shown as fold change $\Delta F/F_0$, $\Delta F=(F-F_0)$. F_0 was calculated as the mean fluorescence of the cell soma of the md-L neuron for five frames (1.6 frames/sec) prior to initiating the stimuli. The pseudo color images of GCaMP6f or tdTomato in the cell soma of the md-L neurons were prepared using image J software (https://imagej.nih.gov/ij/) with the 16 color LUT tool.

Mechanical response recordings—We recorded mechanically-induced action potentials from md-L neurons by performing single-unit recordings similar to the protocol that we described previously[7] with modifications. 1-day old flies were immobilized by impaling them with a long-tapered, sharp glass pipet (length, 76 mm, tip size < 1 μm; tip taper length, 5 mm) from the thorax through the proboscis so that the proboscis was fully extended. The preparation was secured on a glass slide and the lateral side of the labellum was flattened on the surface of the slide. We located the soma of md-L neurons by examining GFP fluorescence due to expression of *UAS-GFP* under the control of *tmc-Gal4* or *tmc-QF* driver. We placed the sharp recording glass pipet in close vicinity to the soma of the md-L neurons. The reference electrode was attached to the root of the proboscis containg a small amount of electrode cream (SignaCreme). The impaling glass pipet, recording and reference electrodes were filled with Ringer's solution (140 mM NaCl, 3 mM $MgCl^2$, 2 mM $CaC1^2$, 10 mM D-glucose, 10 mM HEPES, pH 7.4).

We applied mechanical force using a sealed glass pipet attached to a piezoelectric system by pushing the cuticle area in between S6 and L8 for a travel distance of 10 μm or 20 μm. The signals were collected and amplified 10-fold using a signal connection interface box (Syntech, universal single ended probe) and were filtered between a high cutoff at 3,000 Hz and a low cutoff at 200 Hz. The filtered spikes were acquired and analyzed using AutoSpike software (Syntech).

Hair bending angle analyses—To determine the extent of bending due to application of sucrose only or sucrose plus particles we trapped individual flies in a cutoff pipet tip (Olympus 200 μL Reach Tip, 24-150RL) with only the labellum exposed. The balls of 50 mM sucrose solution or 50 mM sucrose plus 10% 9.2 μm particles at the end of a pipet (Olympus 10 μL Reach Tip, 24-121RL) were applied to the fly labellum. We videotaped the event before and during contact of the labellum using a digital camera (Axiocam 506 color,

Author Manuscript Author Manuscript Author Manuscript Author Manuscript

Zeiss Axio Zoom.V16) at a frame rate of 5 fps (0.2 s per frame). The bendings of L-type hairs were assessed by superimposing a straight line over the sensilla and determining the angle between the two lines before and after the food contact event in consecutive frames using Adobe illustrator software.

Multiple protein sequences alignment—The protein sequences for *Arabidopsis thaliana* OSCA1.1 (At4g04340), *Homo sapien* TMEM63A (NP_055513.2, NM_014698.3), *Mus musculus* TMEM63A (NP_659043.1, NM_144794.2), *Aedes aegypti* TMEM63 (AAEL010404-PA) were downloaded from the NCBI protein database. The sequence for *Drosophila melanogaster* TMEM63 (coding gene, *Dmel_CG11210*, FBpp0087859) was downloaded from Flybase. The protein sequences alignments and guide tree were analyzed using Clustal Omega(https://www.ebi.ac.uk/Tools/msa/clustalo/), and edited using Jalview.[42] The 11 transmembrane domains in TMEM63 were predicted by the Protter online analysis program (http://wlab.ethz.ch/protter/start/).

Viscosity measurements—Viscosities were measured by immersing the sensor from a Viscolite 700HP bench viscometer (Material Research Laboratory, University of California, Santa Barbara) into each solution. The tip of the sensor vibrated in the fluid thereby detecting the shearing forces in the fluid and allowing us to assess the viscosity of the liquid. Solutions with 1–10% (w/v) particles were prepared by adding silica microspheres (Monodisperse Silica Microspheres, 9.2 μm diameter, Cospheric, Co.) into a 50 mM sucrose solution. We vortexed the mixtures thoroughly before measuring. The readings remained constant for at least 2 min. The 0.25–1.5% HPC solution (w/v), were prepared by adding HPC powder (Sigma Aldrich, 191906-100G) to 50 mM sucrose solution in a 50 mL tube at room temperature. We dissolved the HPC thoroughly by gently rotating the tubes overnight.

QUANTIFICATION AND STATISTICAL ANALYSIS

Descriptions, results and sample sizes of each test are provided in the Figure legends. All replicates with flies were biological replicates using different animals. Data for all quantitative experiments were collected on at least three different days. For the PER behavioral experiments each “n” represents a single test performed with ≥12 animals. Based on our experience and common practices in this field, we used a sample size of n=5 trials for each genotype or treatment. Each trial employed ≥12 flies. Each “n” for the Ca^{2+} imaging and electrophysiological recording experiments represents an analysis of a single, independent fly (n = 7–8). Each “n” for the bending angle analyses represents one L-type hair. A total of 5 animals with 4 L-type hairs from each were analyzed for each sample. Error bars represent the standard errors of the means (SEMs). Statistical tests were performed using GraphPad Prism 7 software. We used nonparametric Mann-Whitney tests with the Wilcoxon rank sum test to compare two groups of data (e.g. non-particle versus food with particles of the same genotype). We set the significance level, a = 0.05 and power, 1-b = 0.9. Asterisks indicate statistical significance: *p < 0.05, **p < 0.01, and ***p < 0.001.

Author Manuscript Author Manuscript Author Manuscript Author Manuscript

Supplementary Material

Refer to Web version on PubMed Central for supplementary material.

Acknowledgments

We thank Dhananjay Thakur for discussions and technical support, Geoff Meyerhof and Dhananjay Thakur for comments on the manuscript, and Junjie Luo for the pw35-P2A::Gal4 plasmid. This work was supported by grants to CM from the National Institute on Deafness and Other Communication Disorders (DC007864 and DC016278).

References

1. Montell C (2021). *Drosophila* sensory receptors—a set of molecular Swiss Army Knives. Genetics *(in press)*.
2. Liman ER, Zhang YV, and Montell C (2014). Peripheral coding of taste. Neuron 81, 984–1000. [PubMed: 24607224]
3. Kinnamon SC, and Finger TE (2019). Recent advances in taste transduction and signaling. F1000Research 8.
4. Szczesniak AS (2002). Texture is a sensory property. Food Qual. Prefer. 13, 215–225.
5. Sánchez-Alcañiz JA, Zappia G, Marion-Poll F, and Benton R (2017). A mechanosensory receptor required for food texture detection in *Drosophila*. Nat Commun 8, 14192. [PubMed: 28128210]
6. Jeong YT, Oh SM, Shim J, Seo JT, Kwon JY, and Moon SJ (2016). Mechanosensory neurons control sweet sensing in *Drosophila*. Nat Commun 7, 12872. [PubMed: 27641708]
7. Zhang YV, Aikin TJ, Li Z, and Montell C (2016). The basis of food texture sensation in *Drosophila*. Neuron 91, 863–877. [PubMed: 27478019]
8. Li Q, DeBeaubien NA, Sokabe T, and Montell C (2020). Temperature and sweet taste integration in *Drosophila*. Curr. Biol. 30, 2051–2067 [PubMed: 32330421]
9. Cook KLK, and Hartel RW (2010). Mechanisms of Ice Crystallization in Ice Cream Production. Compr Rev Food Sci F 9, 213–222.
10. Breen SP, Etter NM, Ziegler GR, and Hayes JE (2019). Oral somatosensatory acuity is related to particle size perception in chocolate. Sci. Rep. 9, 7437. [PubMed: 31092875]
11. Tyle P (1993). Effect of size, shape and hardness of particles in suspension on oral texture and palatability. Acta Psychol. (Amst.) 84, 111–118. [PubMed: 8237451]
12. Mansourian S, Enjin A, Jirle EV, Ramesh V, Rehermann G, Becher PG, Pool JE, and Stensmyr MC (2018). Wild African *Drosophila melanogaster* are seasonal specialists on marula fruit. Curr. Biol. 28, 3960–3968 e3963. [PubMed: 30528579]
13. Dweck HK, Ebrahim SA, Kromann S, Bown D, Hillbur Y, Sachse S, Hansson BS, and Stensmyr MC (2013). Olfactory preference for egg laying on citrus substrates in *Drosophila*. Curr. Biol. 23, 2472–2480. [PubMed: 24316206]
14. Simao RA, Silva AP, Peroni FH, do Nascimento JR, Louro RP, Lajolo FM, and Cordenunsi BR (2008). Mango starch degradation. I. A microscopic view of the granule during ripening. J Agric Food Chem 56, 7410–7415. [PubMed: 18656941]
15. Li D, and Zhu F (2018). Starch structure in developing kiwifruit. Int. J. Biol. Macromol. 120, 1306–1314. [PubMed: 30172805]
16. Zakhartsev M, and Reuss M (2018). Cell size and morphological properties of yeast Saccharomyces cerevisiae in relation to growth temperature. FEMS Yeast Res. 18.
17. Yuan F, Yang H, Xue Y, Kong D, Ye R, Li C, Zhang J, Theprungsirikul L, Shrift T, Krichilsky B, et al. (2014). OSCA1 mediates osmotic-stress-evoked Ca^{2+} increases vital for osmosensing in *Arabidopsis*. Nature 514, 367–371. [PubMed: 25162526]
18. Hou C, Tian W, Kleist T, He K, Garcia V, Bai F, Hao Y, Luan S, and Li L (2014). DUF221 proteins are a family of osmosensitive calcium-permeable cation channels conserved across eukaryotes. Cell Res. 24, 632–635. [PubMed: 24503647]

Author Manuscript Author Manuscript Author Manuscript Author Manuscript

19. Zhang M, Wang D, Kang Y, Wu JX, Yao F, Pan C, Yan Z, Song C, and Chen L (2018). Structure of the mechanosensitive OSCA channels. Nat. Struct. Mol. Biol. 25, 850–858. [PubMed: 30190597]
20. Murthy SE, Dubin AE, Whitwam T, Jojoa-Cruz S, Cahalan SM, Mousavi SAR, Ward AB, and Patapoutian A (2018). OSCA/TMEM63 are an Evolutionarily Conserved Family of Mechanically Activated Ion Channels. eLife 7, e41844. [PubMed: 30382938]
21. Shiraiwa T, and Carlson JR (2007). Proboscis extension response (PER) assay in Drosophila. J. Vis. Exp 193, doi: 10.3791/3193.
22. Kim SE, Coste B, Chadha A, Cook B, and Patapoutian A (2012). The role of *Drosophila* Piezo in mechanical nociception. Nature 483, 209–212. [PubMed: 22343891]
23. Walker RG, Willingham AT, and Zuker CS (2000). A *Drosophila* mechanosensory transduction channel. Science 287, 2229–2234. [PubMed: 10744543]
24. Gong Z, Son W, Chung YD, Kim J, Shin DW, McClung CA, Lee Y, Lee HW, Chang DJ, Kaang BK, et al. (2004). Two interdependent TRPV channel subunits, Inactive and Nanchung, mediate hearing in *Drosophila*. J. Neurosci. 24, 9059–9066. [PubMed: 15483124]
25. Kim J, Chung YD, Park DY, Choi S, Shin DW, Soh H, Lee HW, Son W, Yim J, Park CS, et al. (2003). A TRPV family ion channel required for hearing in *Drosophila*. Nature 424, 81–84. [PubMed: 12819662]
26. Hiroi M, Marion-Poll F, and Tanimura T (2002). Differentiated response to sugars among labellar chemosensilla in *Drosophila*. Zoolog. Sci. 19, 1009–1018. [PubMed: 12362054]
27. Falk R, Bleiser-Avivi N, and Atidia J (1976). Labellar taste organs of *Drosophila melanogaster*. J. Morph. 150, 327–341. [PubMed: 30261703]
28. Haj-Ahmad Y, and Hickey DA (1982). A molecular explanation of frequency-dependent selection in Drosophila. Nature 299, 350–352. [PubMed: 6180326]
29. Ballesteros A, Fenollar-Ferrer C, and Swartz KJ (2018). Structural relationship between the putative hair cell mechanotransduction channel TMC1 and TMEM16 proteins. Elife 7, e38433. [PubMed: 30063209]
30. Pan B, Akyuz N, Liu XP, Asai Y, Nist-Lund C, Kurima K, Derfler BH, Gyorgy B, Limapichat W, Walujkar S, et al. (2018). TMC1 forms the pore of mechanosensory transduction channels in vertebrate inner ear hair cells. Neuron 99, 736–753 e736. [PubMed: 30138589]
31. Jojoa-Cruz S, Saotome K, Murthy SE, Tsui CCA, Sansom MS, Patapoutian A, and Ward AB (2018). Cryo-EM structure of the mechanically activated ion channel OSCA1.2. eLife 7, e41845. [PubMed: 30382939]
32. Weiss LA, Dahanukar A, Kwon JY, Banerjee D, and Carlson JR (2011). The molecular and cellular basis of bitter taste in *Drosophila*. Neuron 69, 258–272. [PubMed: 21262465]
33. Cameron P, Hiroi M, Ngai J, and Scott K (2010). The molecular basis for water taste in *Drosophila*. Nature 465, 91–95. [PubMed: 20364123]
34. Toda H, Zhao X, and Dickson BJ (2012). The *Drosophila* female aphrodisiac pheromone activates *ppk23*$^{+}$ sensory neurons to elicit male courtship behavior. Cell Rep. 1, 599–607. [PubMed: 22813735]
35. Sweeney ST, Broadie K, Keane J, Niemann H, and O'Kane CJ (1995). Targeted expression of tetanus toxin light chain in Drosophila specifically eliminates synaptic transmission and causes behavioral defects. Neuron 14, 341–351. [PubMed: 7857643]
36. Yavuz A, Jagge C, Slone J, and Amrein H (2014). A genetic tool kit for cellular and behavioral analyses of insect sugar receptors. Fly 8, 189–196. [PubMed: 25984594]
37. Thistle R, Cameron P, Ghorayshi A, Dennison L, and Scott K (2012). Contact chemoreceptors mediate male-male repulsion and male-female attraction during *Drosophila* courtship. Cell 149, 1140–1151. [PubMed: 22632976]
38. Wang Z, Singhvi A, Kong P, and Scott K (2004). Taste representations in the *Drosophila* brain. Cell 117, 981–991. [PubMed: 15210117]
39. Gong WJ, and Golic KG (2003). Ends-out, or replacement, gene targeting in *Drosophila*. Proc. Natl. Acad. Sci. USA 100, 2556–2561. [PubMed: 12589026]
40. Moon SJ, Lee Y, Jiao Y, and Montell C (2009). A *Drosophila* gustatory receptor essential for aversive taste and inhibiting male-to-male courtship. Curr. Biol. 19, 1623–1627. [PubMed: 19765987]

Author Manuscript Author Manuscript Author Manuscript Author Manuscript

41. Zimmerman SG, Peters NC, Altaras AE, and Berg CA (2013). Optimized RNA ISH, RNA FISH and protein-RNA double labeling (IF/FISH) in *Drosophila* ovaries. Nat. Protoc 8, 2158–2179. [PubMed: 24113787]

42. Waterhouse AM, Procter JB, Martin DM, Clamp M, and Barton GJ (2009). Jalview Version 2--a multiple sequence alignment editor and analysis workbench. Bioinformatics 25, 1189–1191. [PubMed: 19151095]

Author Manuscript Author Manuscript Author Manuscript Author Manuscript

Highlights

- Flies prefer feeding on foods containing particles of a certain size
- Sensation of particles in food depends on the OSCA/TMEM63 channel
- TMEM63 detects particles in food through subtle deflections of taste sensilla
- Mild deflections of sensilla require TMEM63 for activation of md-L neurons

Author Manuscript Author Manuscript Author Manuscript Author Manuscript

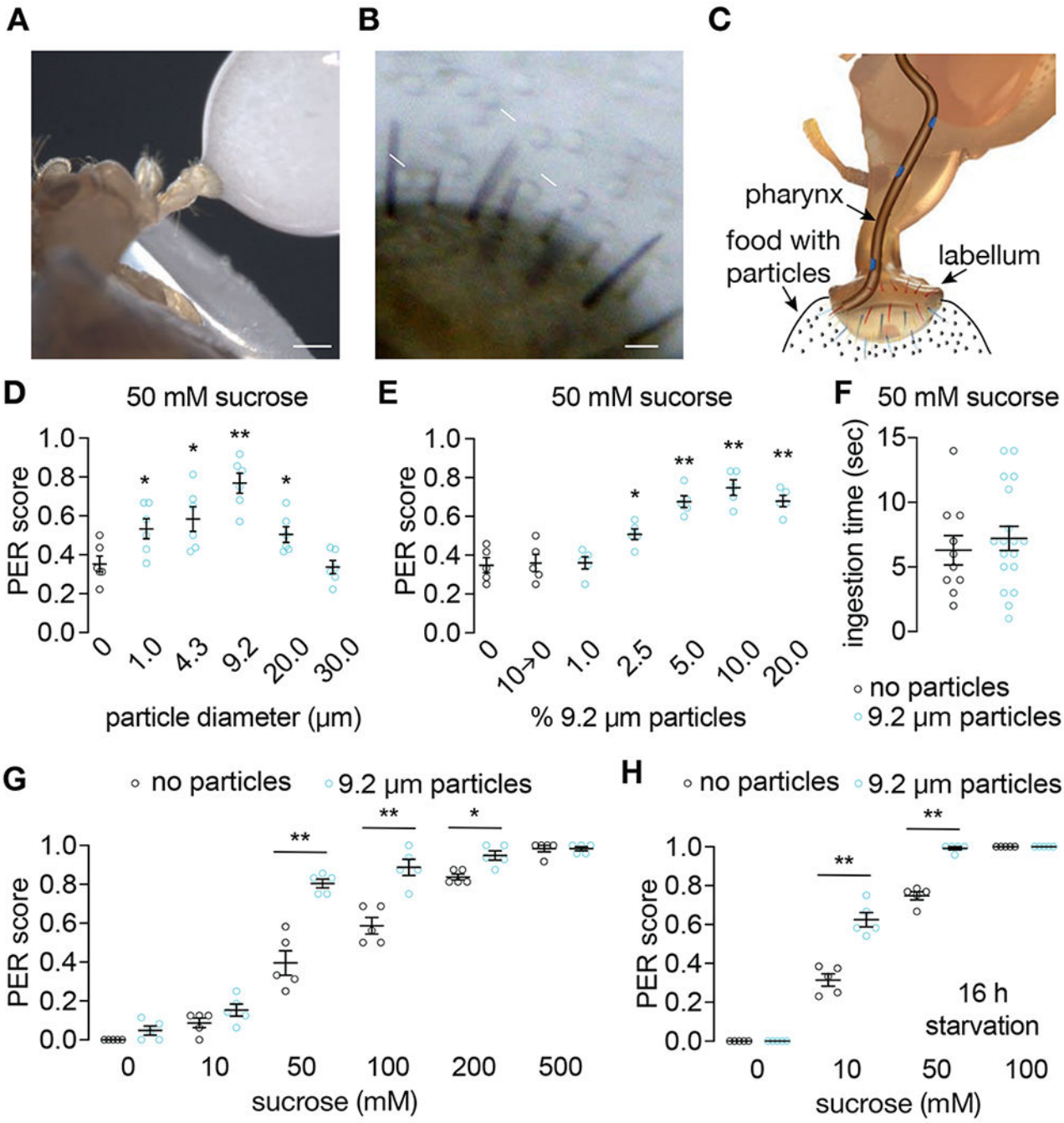

Figure 1. Influence of particles size on sucrose acceptance.

(A) Fly extending proboscis after contact with 50 mM sucrose solution containing 9.2 μm particles (10% w/v). Scale bars in **A** and **B**: 250 μm.

(B) 9.2 μm particles (10% w/v) contacting sensilla on the labellum. Arrows indicate examples of particles.

(C) Cartoon depicting a labellum contacting food containing particles. Cuticle is partially removed exposing the pharynx with internal neurons (blue).

Author Manuscript Author Manuscript Author Manuscript Author Manuscript

(D–G) PER assays performed on control (w^{1118}) flies starved for 2 hrs. Proboscis extension for ≥1 second is scored as 1.0, the score is 0.5 if the extension is <1 second, and no extension is 0. **D**, PERs to 50 mM sucrose alone (0 particle diameter) relative to sucrose containing particles of different sizes (1.0 – 30.0 μm; 10% w/v). **E**, PERs6 to 50 mM sucrose alone versus sucrose plus different concentrations of 9.2 μm particles (0 – 20% w/v). 10→0; sucrose incubated with 10% particles, which were then removed. **F**, Ingestion time of responsive flies to 50 mM sucrose alone (n=10) or 50 mM sucrose containing 9.2 μm particles (10% w/v; n=18). **G**, PERs using 0 – 500 mM sucrose alone (black data points) versus the same percentages of sucrose solution mixed with 9.2 μm particles (10% w/v; cyan data points). See also Figure S1A.

(H) PERs using control flies (starved for 16 h) using the indicated percentages of sucrose alone or sucrose plus 9.2 μm particles (10% w/v).

Means ±SEMs. *P<0.05, **P<0.01. n=5 trials. ≥12 flies/trial. Non-parametric Mann-Whitney tests were performed between particle group (cyan circles) and control non-particle group (black circles).

Author Manuscript Author Manuscript Author Manuscript Author Manuscript

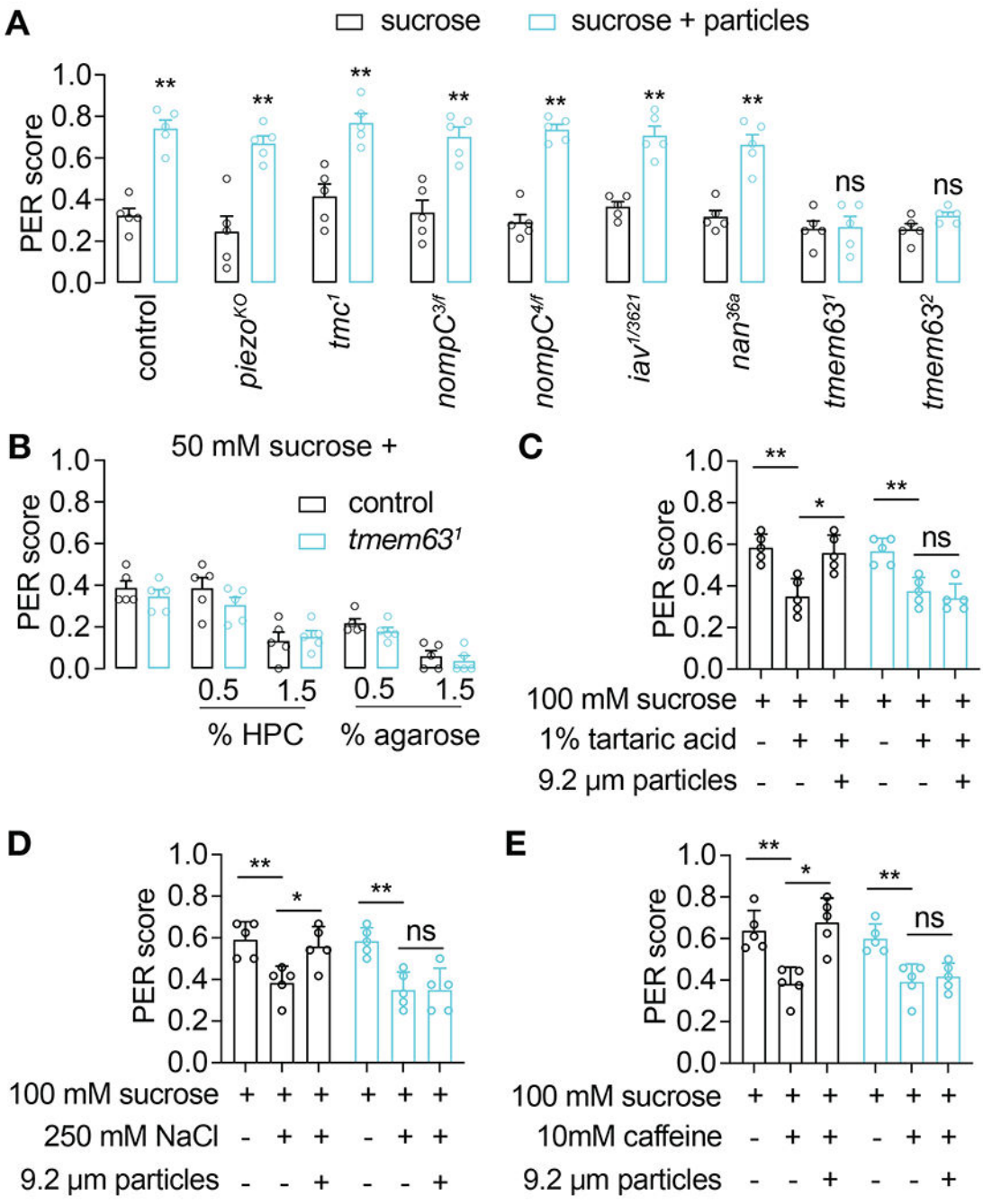

Figure 2. Mutation of *tmem63* impairs appeal of particles in food.

(A) Effects of mutations disrupting mechanosensory channels on increased acceptance of sucrose containing 9.2 μm particles (10% w/v) versus sucrose alone. Tests employed 50 mM sucrose except for 300 mM for *nan*^{36a} due to decreased sucrose attraction by *nan*^{36a}. Statistical tests were between flies offered sucrose alone (black) or sucrose plus particles (cyan). See also Figure S1A.

(B) PERs comparing responses to different viscosities and hardness. Statistical tests were between control flies (black) and *tmem63*^{1} (cyan).

Author Manuscript Author Manuscript Author Manuscript Author Manuscript

(C) PERs comparing control flies and *tmem63*^{1} using 100 mM sucrose and 1% tartaric acid in the presence or absence of particles.
(D) PERs comparing control flies and *tmem63*^{1} responses to 100 mM sucrose and 250 mM NaCl in the presence or absence of particles.
(E) PERs comparing control flies and *tmem63*^{1} responses to 100 mM sucrose and 10 mM caffeine in the presence or absence of particles.
Means ±SEM. *P<0.05, **P<0.01. n=5 trials. ≥12 flies/trial. Nonparametric Mann-Whitney tests, ns, not significant.
See Figures S1B—S1D and S2.

Author Manuscript Author Manuscript Author Manuscript Author Manuscript

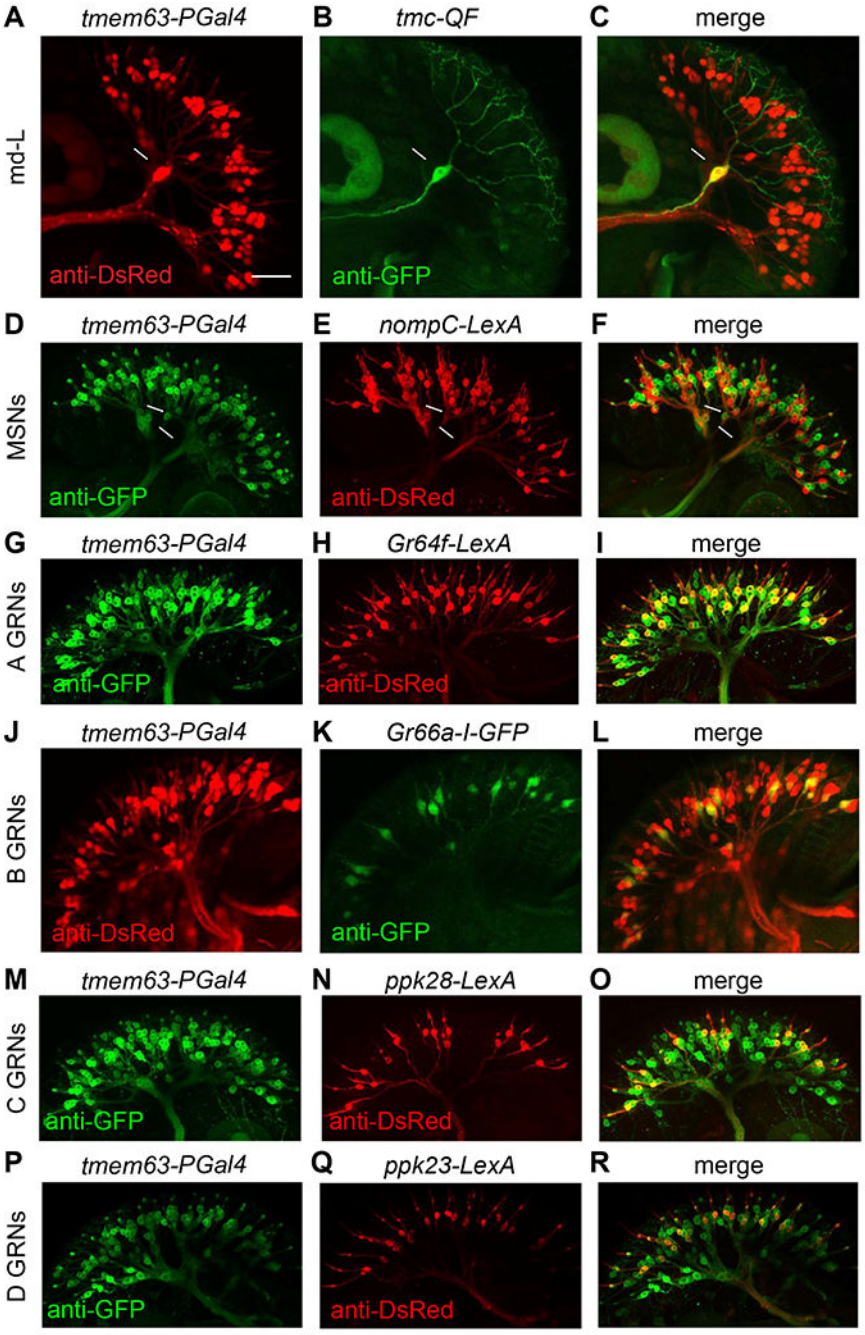

Figure 3. Expression of *tmem63-PGal4* reporter in the labellum.

Overlap between the *tmem63-PGal4* reporter (*tmem63-PGal4/+* flies) and the indicated reporters. Scale bar, 20 μm.

(A–C) Double labeling with md-L reporter (*tmc-QF*). Genotype: *tmem63-PGal4/tmc-QF;QUAS-mCD8::GFP/UAS-tdTomato*. **A**, Anti-DsRed. **B**, Anti-GFP. **C**, Merge of **A** and **B**.

(D–F) Double labeling with MSN reporter (*nompC-LexA*). The arrows indicate neurons projecting to two short poreless mechanosensory sensilla. Genotype: *tmem63-PGal4/*

Author Manuscript Author Manuscript Author Manuscript Author Manuscript

LexAop-rCD2::RFP,UAS-mCD8::GFP;nompC-LexA/+. **D**, Anti-GFP. **E**, Anti-DsRed. **F**, Merge of **D** and **E**.

(G–I) Double labeling with A GRN reporter (*Gr64f-LexA*). Genotype: *tmem63-PGal4/ LexAop-rCD2::RFP, UAS-mCD8::GFP;Gr64f-LexA/+*. **G**, Anti-GFP. **H**, Anti-DsRed. **I**, Merge of *G* and **H.**

(J–L) Double labeling with B GRN reporter (*Gr66a-I-GFP*). Genotype: *tmem63-PGal4/+;Gr66-I-GFP/UAS-tdTomato*. **J**, Anti-DsRed. **K**, Anti-GFP. **L**, Merge of **J** and **K.**

(M–O) Double labeling with C GRN reporter (*ppk28-LexA*). Genotype: *tmem63-PGal4/ LexAop-rCD2::RFP, UAS-mCD8::GFP;ppk28-LexA/+*. **M**, Anti-GFP. **N**, Anti-DsRed. **O**, Merge of **M** and **N**.

(P–R) Double labeling with D GRN reporter (*ppk23-LexA*). Genotype: *tmem63-PGal4/ LexAop-rCD2::RFP, UAS-mCD8::GFP;ppk23-LexA/+*. **P**, Anti-GFP. **Q**, Anti-DsRed. **R**, Merge of **P** and **Q**.

See Figure S3.

Author Manuscript Author Manuscript Author Manuscript Author Manuscript

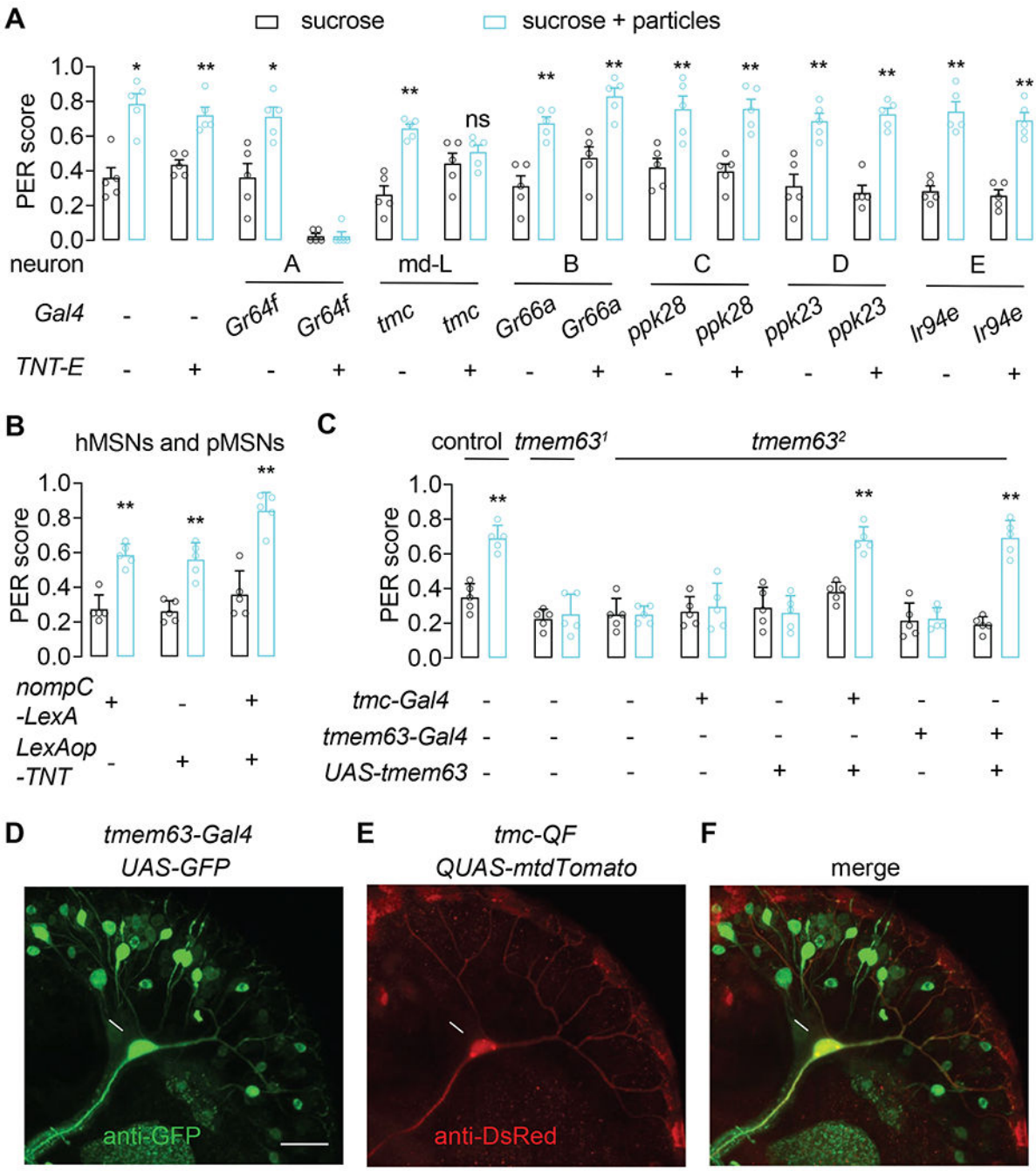

Figure 4. *tmem63* required specifically in md-L for the appeal of particles in food.

(A) PERs after inhibiting different neuron classes with *UAS-TNT-E* and the indicated Gal4. PERs using 50 mM sucrose alone or sucrose plus 9.2 μm particles (10% w/v).

(B) PERs after inhibiting MSNs in hairs and pegs (hMSNs & pMSNs). Assays were performed using 50 mM sucrose (black) or sucrose plus 9.2 μm particles (10% w/v; cyan).

(C) Testing for rescue of the *tmem63*^{2} phenotype by expressing *UAS-tmem63* or *UAS-tmc* under control of the *tmem63-Gal4* or the *tmc-Gal4*. n=5 trials. ≥12 flies/trial. Means ±SEMs. *P<0.05, **P<0.01. ns, not significant. Non-parametric Mann-Whitney tests were

Author Manuscript Author Manuscript Author Manuscript Author Manuscript

performed between sucrose only (black) and sucrose plus particles (cyan) of each genotype for A–C.

(D–F) Overlap between *tmem63-Gal4* and *tmc-QF* in md-L. Genotype: *UAS-GFP/tmc-QF;QUAS-mtdTomato/tmem63-Gal4*. **D**, Anti-GFP. **E**, Anti-DsRed. **F**, Merge of **D** and **E**. See Figure S4.

Author Manuscript Author Manuscript Author Manuscript Author Manuscript

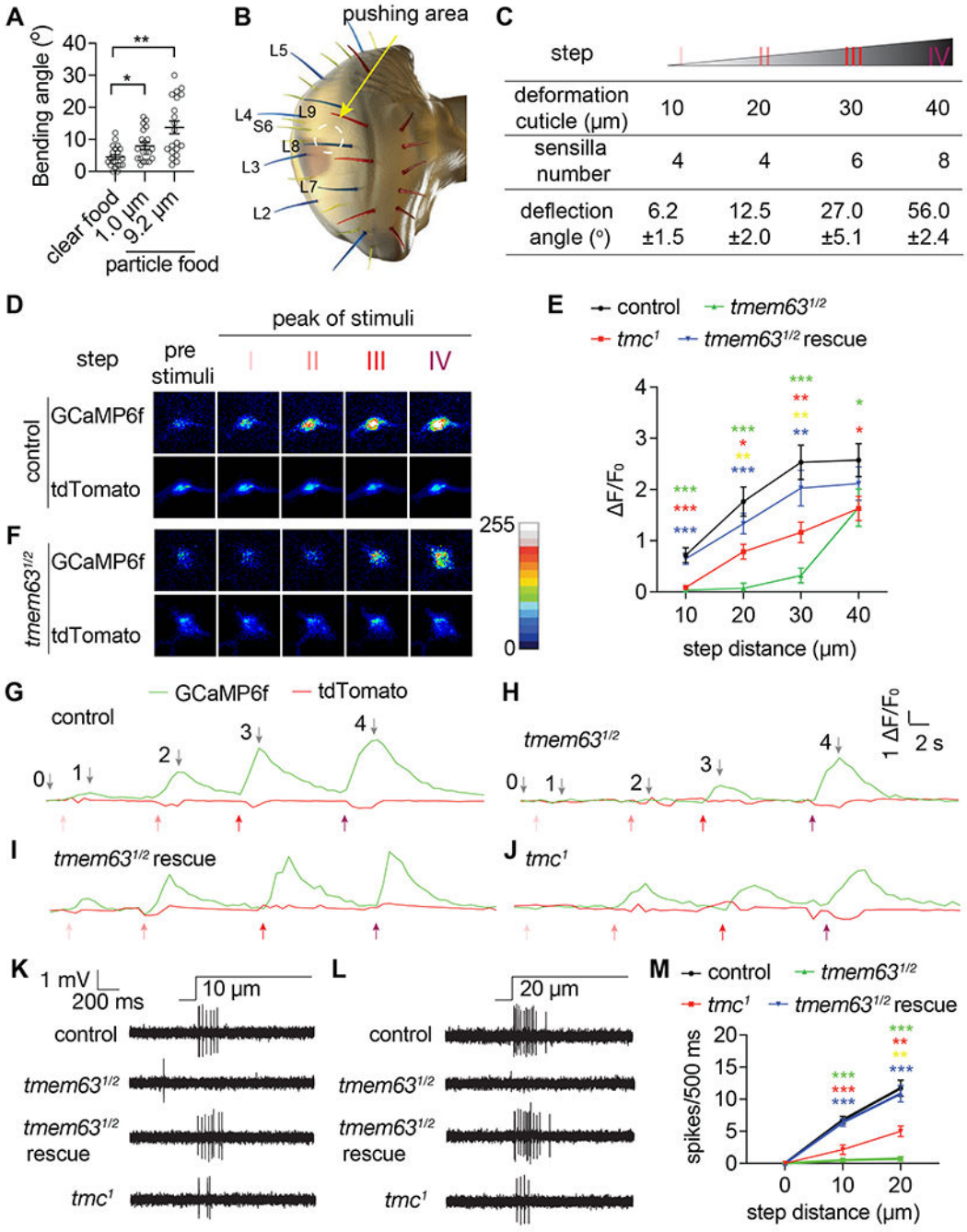

Figure 5. *tmem63* required in md-L for sensing gentle deflections of sensilla.

(A) Deflection angles of L-type sensilla upon contact with 50 mM sucrose (clear food), 50 mM sucrose plus 1.0 μm, or 9.2 μm particles (10% w/v; particle food). n= 20; 4.0 ±0.3 L-type sensilla per n.

(B) Pushing area (dashed circle) in the labellum. Sensilla type: L, blue; I, red; S, yellow. Numbering for L-type sensilla and S6 are as described.[32]

(C) Deflection angles of sensilla using different levels of deformation of the labellum in the area indicated in **B** (dashed circle).

Author Manuscript Author Manuscript Author Manuscript Author Manuscript

(D) GCaMP6f responses ($\Delta F/F_0$) of md-L from a single control labellum to four levels of mechanical stimuli (I-IV). tdTomato was co-expressed as an internal control. Genotype: *tmc-Gal4/UAS-GCaMP6f,UAS-tdTomato*. Pseudo color of GCaMP6f and tdTomato pre-stimulation (0) and at the four peak levels of mechanical stimulation (1–4). Scale bar, 20 μm.
(E) Peak $\Delta F/F_0$ in response to mechanical stimuli. n= 7–8. Comparisons: control versus $tmem63^{1/2}$ (green), control versus $tmcw^{1}$ (red), $tmem63^{1/2}$ versus $tmem63^{1/2}$ rescue (blue), and $tmem63^{1/2}$ versus tmc^{1} (yellow).
(F) GCaMP6f responses ($\Delta F/F_0$) of md-L from a single $tmem63^{1/2}$ labellum to four levels of mechanical stimuli. tdTomato was an internal control. Genotype: *tmc-QF,*$tmem63^{2}$*/UAS-GCaMP6f,UAS-tdTomato,*$tmem63^{1}$*;QUAS-Gal4/+*. Pseudo color of GCaMP6f and tdTomato pre-stimuli (0) and at peak levels of mechanical stimulation (1–4). Scale bar, 20 μm.
(G—J) $\Delta F/F_0$ traces showing changes of GCaMP6f fluorescence in md-L in response to four levels of mechanical stimuli (pink, red and purple arrows). $\Delta F/F_0$ prior to stimuli (0) and the peak $\Delta F/F_0$ at the four levels of mechanical stimuli (grey arrows; 1–4) are indicated. **G**, Control. **H**, $tmem63^{1/2}$. **I**, Testing for rescue of $tmem63^{1/2}$ defect by expressing *UAS-tmem63* in md-L. Genotype: *tmc-QF,*$tmem63^{2}$*/UAS-GCaMP6f,UAS-tdTomato,*$tmem63^{1}$*;QUAS-Gal4/UAS-tmem63*. **J**, tmc^{1}.
(K, L) Extracellular recordings of md-L responses to 10 μm or 20 μm cuticle deformation. Genotype of rescue flies: *tmc-QF,*$tmem63^{2}$*/UAS-GFP,*$tmem63^{1}$*;QUAS-Gal4/UAS-tmem63*. **K**, 10 μm deformation. **L**, 20 μm deformation.
(M) Spikes/500 ms. n= 7–8. Comparisons: control versus $tmem63^{1/2}$ (black), control versus tmc^{1} (red), $tmem63^{1/2}$ versus $tmem63^{1/2}$ rescue (blue), and $tmem63^{1/2}$ versus tmc^{1} (yellow). Means ±SEMs. *P<0.05, **P<0.01, ***P<0.001. Non-parametric Mann-Whitney tests were performed between two groups.
See Figure S5.

Author Manuscript Author Manuscript Author Manuscript Author Manuscript

Table 1.

Neurons labeled by the *tmem63-PGal4* and the *tmem63-Gal4*.

Shown are the number of neurons labeled by the indicated markers and by the *tmem63-PGal4* and the *tmem63-Gal4*. Abbreviations: MSN, mechanosensory neuron; hMSN, hairless MSN; pMSN, peg MSN; pmMSN, poreless mechanosensory MSN; PM sensilla, poreless, mechanosensory sensilla.

Organ	Neuron	Former name of neuron	Marker	No. neurons labeled by marker	No. neurons labeled by *tmem63-PGal4*	No. neurons labeled by *tmem63-Gal4*
	md-L		*tmc-QF*	1.0 ±0.0	1.0 ±0.0	1.0 ±0.0
External taste sensilla						
	hMSN		*nompC-LexA*	30.0 ±0.5	0.0 ±0.0	1.7 ±0.3
	A	sugar	*Gr64f-LexA*	40.0 ±1.7	40.0 ±1.7	1.4 ±0.6
	B	bitter	*Gr66a-I-LexA*	28.7 ±0.9	28.7 ±0.9	10.0 ±1.5
	C	water	*ppk28a-LexA*	11.6 ±1.2	11.6 ±1.2	0.7 ±0.5
	D	cation	*ppk23a-LexA*	19.0 ±0.8	19.0 ±0.8	8.3 ±4.5
Taste pegs						
	pMSN		*nompC-LexA*	33.3 ±0.3	6.0 ±0.6	0.0 ±0.0
	GRN		*Ir76b-QF*	37.3 ±2.3	26.0 ±0.6	30.3 ±1.4
PM sensilla	pmMSN		*nompC-LexA*	2.0 ±0.0	2.0 ±0.0	0.0 ±0.0

Author Manuscript Author Manuscript Author Manuscript Author Manuscript

KEY RESOURCES TABLE

REAGENT or RESOURCE	SOURCE	IDENTIFIER
Antibodies		
anti-GFP (mouse)	Invitrogen	Cat # A-11120 RRID: AB_221568
anti-DsRed antibody (rabbit)	Clontech Laboratories, Inc.	Cat # 632496 RRID: AB_10013483
Goat anti-mouse, Alexa Fluor 488	Thermo Fisher Scientific	Cat # A-11001 RRID: AB_2534069
Goat anti-rabbit, Alexa Fluor 568	Thermo Fisher Scientific	Cat # A-11036 RRID: AB_10563566
biotin-conjugated digoxigenin	Jackson ImmunoResearch Laboratories	Cat # 200-062-156 RRID: AB_2339017
Chemicals		
Sucrose	Sigma-Aldrich	Cat # S0389
Monodisperse silica microspheres, diameter 1.0 μm	NanoXact, Co.	Cat # SISD1000
Monodisperse silica microspheres, diameter 4.3 μm	Cospheric, Co.	Cat # SiO2MS-2.0 4.3um
Monodisperse silica microspheres, diameter 9.2 μm	Cospheric, Co.	Cat # SiO2MS-2.0 9.2um
Monodisperse silica microspheres, diameter 20 μm	EPRUI Biotech, Co.	Cat # 2-001-20
Monodisperse silica microspheres, diameter 30 μm	Cospheric, Co.	Cat # S-SLGMS-2.5 29-32um
Hydroxypropyl cellulose	Sigma-Aldrich	Cat # 191906
Agarose	Life Technologies	Cat # 16500500
PBS	Fisher Scientific	Cat # AAJ62036K2
DEPC treated water	Thermo Fisher	Cat # AM9920
Formamide	Sigma	Cat # F9037
SSC	Sigma	Cat # P9416
tRNA	Thermo Fisher	Cat # 15401029
Salmon sperm DNA	Sigma	Cat # D1626
Paraformaldehyde	Electron Microscopy Sciences	
Triton X-100	Sigma	Cat # X100
VECTASHIELD anti-fade mounting media	Vector Labs	Cat # H-1200
Silicone lubricant	Dow Corning	Cat # DC976
Electrode cream	SignaCreme	Cat # 17-05
Experimental Models: Organisms/Strains		
Drosophila: w^{1118}	Bloomington Drosophila Stock Center	Cat # BL5905
Drosophila: tmem63^{1}	In this paper	NA
Drosophila: tmem63^{2}	In this paper	NA
Drosophila: tmem63-PGal4	In this paper	NA
Drosophila: tmem63-Gal4	In this paper	NA
Drosophila: UAS-tmem63	In this paper	NA
Drosophila: Gr66a-Gal4 (chromosome 2 insertion)	From H. Amrein	NA

Author Manuscript Author Manuscript Author Manuscript Author Manuscript

REAGENT or RESOURCE	SOURCE	IDENTIFIER
Drosophila: Gr66a-Gal4 (chromosome 3 insertion)	Bloomington Drosophila Stock Center	Cat # BL57670
Drosophila: Gr64f-Gal4	Bloomington Drosophila Stock Center	Cat # BL57669
Drosophila: UAS-TNT-E	[35]	NA
Drosophila: ppk28-Gal4	[33]	NA
Drosophila: ppk23-Gal4	[34]	NA
Drosophila: TMC-Gal4	[7]	NA
Drosophila: TMC-QF	[7]	NA
Drosophila: Ir94e-Gal4	Bloomington Drosophila Stock Center	Cat # BL81246
Drosophila: UAS-tdTomato	Bloomington Drosophila Stock Center	Cat # BL36327
Drosophila: QUAS-Gal4	Bloomington Drosophila Stock Center	Cat # BL83132
Drosophila: QUAS-mtdTomato	Bloomington Drosophila Stock Center	Cat # BL30004
Drosophila: UAS-GFP	Bloomington Drosophila Stock Center	Cat # BL52261
Drosophila: $nompC^{3}$	[23]	NA
Drosophila: $nompC^{4}$	[23]	NA
Drosophila: $nompC^{f00642}$	Bloomington Drosophila Stock Center	Cat # BL85609
Drosophila: $piezo^{KO}$	Bloomington Drosophila Stock Center	Cat # BL58770
Drosophila: iav^{3621}	[24]	NA
Drosophila: iav^{1}	Kyoto Stock Center	Cat # 101174
Drosophila: nan^{36a}	[25]	NA
Drosophila: UAS-tdTomato	Bloomington Drosophila Stock Center	Cat # BL36328
Drosophila: LexAop-TNT	From Chi-Hon Lee	NA
Drosophila: UAS-GCaMP6f	Bloomington Drosophila Stock Center	Cat # BL42747
Drosophila: nompC-lexA	Bloomington Drosophila Stock Center	Cat # BL52241
Drosophila: LexAop-rCD2::RFP, UAS-mCD8::GFP	Bloomington Drosophila Stock Center	Cat # BL67093
Drosophila: Gr64f-LexA	[36]	NA
Drosophila: ppk23-LexA	From Barry Dickson	NA
Drosophila: ppk28-LexA	[37]	NA
Drosophila: Gr66a-I-GFP	[38]	NA
Drosophila: Ir76b-QF	[7]	NA
Oligonucleotides		
5‘ homology arm for generating *$tmem63^{1}$*. Forward primer: CAGGAGCAGGTCGTTCACAACATTC	This paper	N/A

Author Manuscript Author Manuscript Author Manuscript Author Manuscript

REAGENT or RESOURCE	SOURCE	IDENTIFIER
5‘ homology arm for generating *tmem63*^{1}. Reverse primer: TTCCGACATGACCATGAATTTCACTA	This paper	N/A
3‘ homology arm for generating *tmem63*^{1}. Forward primer: AGAACGCCTACGAATATTATCAGCG	This paper	N/A
3‘ homology arm for generating *tmem63*^{1}. Reverse primer: TATGCTGCGTGCTCAATTCGATGCGG	This paper	N/A
5‘ homology arm for generating *tmem63*^{2}. Forward primer: CATGGTCATGTCGGAAAACAGCAAC	This paper	N/A
5‘ homology arm for generating *tmem63*^{2}. Reverse primer: GGTGCCGCAGAACCGTAAACAA	This paper	N/A
3‘ homology arm for generating *tmem63*^{2}. Forward primer: AGAACGCCTACGAATATTATCAGCG	This paper	N/A
3‘ homology arm for generating *tmem63*^{2}. Reverse primer: TGCGTGATATCATGTTTGACGGACCG	This paper	N/A
5‘ homology arm for generating *tmem63-PGal4*. Forward primer: CACCTGATGGCTGTAATGGCATTG	This paper	N/A
5‘ homology arm for generating *tmem63-PGal4*. Reverse primer: CGCCTCAACACTGTTGACGCTGTA	This paper	N/A
3‘ homology arm for generating *tmem63-PGal4*. Forward primer: CTGCACGCGAAAGCGATAGCAAT	This paper	N/A
3‘ homology arm for generating *tmem63-PGal4*. Reverse primer: GATTACTTGTGGGCAAATCGGCATC	This paper	N/A
Recombinant DNA		
pw35Gal4	[40] Donor vector	N/A
pBPLexA::p65Uw	Donor vector	Addgene Plasmid # 26231
pU6-BbsI-chiRNA	gRNA vector	Addgene Plasmid # 45946
pCS2P+	cDNA vector	Addgene Plasmid # 17095
pUAST	cDNA vector	Brand and Perimon (1993)
Software and Algorithms		
Prism8	Software	https://www.graphpad.com/scientific-software/prism/ RRID:SCR_002798
Fiji	Software	https://imagej.net/Fiji
Other		
DIG RNA Labeling Kit	Roche	Cat # 11175025910
Alexa Fluor™ 488 Tyramide SuperBoost™ Kit, streptavidin	Thermo Fisher	Cat # 40932
Glass capillaries	World Precision Instruments	Cat # 1B150F-3